DENTAL MATERIALS 33 (2017) 99–109

Available online at www.sciencedirect.com

ScienceDirect

journal homepage: www.intl.elsevierhealth.com/journals/dema

Chairside CAD/CAM materials. Part 2: Flexural strength testing

Michael Wendler[a,b], *Renan Belli*[a], *Anselm Petschelt*[a], *Daniel Mevec*[c], *Walter Harrer*[c], *Tanja Lube*[c], *Robert Danzer*[c], *Ulrich Lohbauer*[a,*]

[a] *Friedrich-Alexander Universität Erlangen-Nürnberg (FAU), Zahnklinik 1—Zahnerhaltung und Parodontologie, Forschungslabor für dentale Biomaterialien, Glueckstrasse 11, 91054 Erlangen, Germany*

[b] *Department of Restorative Dentistry, Faculty of Dentistry, University of Concepción, Concepción, Chile*

[c] *Institut für Struktur- und Funktionskeramik, Montanuniversität Leoben, A-8700 Leoben, Austria*

ARTICLE INFO

Article history:
Received 24 October 2016
Accepted 26 October 2016

Keywords:
Biaxial strength
B3B-test
4-point bending
CAD/CAM
Dental ceramics
Resin composites

ABSTRACT

Objective. Strength is one of the preferred parameters used in dentistry for determining clinical indication of dental restoratives. However, small dimensions of CAD/CAM blocks limit reliable measurements with standardized uniaxial bending tests. The objective of this study was to introduce the ball-on-three-ball (B3B) biaxial strength test for dental for small CAD/CAM block in the context of the size effect on strength predicted by the Weibull theory.

Methods. Eight representative chairside CAD/CAM materials ranging from polycrystalline zirconia (e.max ZirCAD, Ivoclar-Vivadent), reinforced glasses (Vitablocs Mark II, VITA; Empress CAD, Ivoclar-Vivadent) and glass-ceramics (e.max CAD, Ivoclar-Vivadent; Suprinity, VITA; Celtra Duo, Dentsply) to hybrid materials (Enamic, VITA; Lava Ultimate, 3M ESPE) have been selected. Specimens were prepared with highly polished surfaces in rectangular plate ($12 \times 12 \times 1.2\,mm^3$) or round disc (Ø = 12 mm, thickness = 1.2 mm) geometries. Specimens were tested using the B3B assembly and the biaxial strength was determined using calculations derived from finite element analyses of the respective stress fields. Size effects on strength were determined based on results from 4-point-bending specimens.

Results. A good agreement was found between the biaxial strength results for the different geometries (plates vs. discs) using the B3B test. Strength values ranged from 110.9 MPa (Vitablocs Mark II) to 1303.21 MPa (e.max ZirCAD). The strength dependency on specimen size was demonstrated through the calculated effective volume/surface.

Significance. The B3B test has shown to be a reliable and simple method for determining the biaxial strength restorative materials supplied as small CAD/CAM blocks. A flexible solution was made available for the B3B test in the rectangular plate geometry.

* *Corresponding author at*: Research Laboratory for Dental Biomaterials, Dental Clinic 1—Operative Dentistry and Periodontology, Glueckstrasse 11, D-91054 Erlangen, Germany. Fax: +49 9131 853 3603.
E-mail address: ulrich.lohbauer@fau.de (U. Lohbauer).

http://dx.doi.org/10.1016/j.dental.2016.10.008

1. Introduction

Strength is the preferred material property used by manufacturers to classify, compare, rank and advertise dental restoratives. Possibly because their target audience are dentists, usually laymen in the affairs of mechanics, fracture strength (σ_f) may get through more easily because of its simple relationship to load (F) capacity (i.e., $\sigma_f \propto F$), a concept of ease clinical applicability: "stronger" materials are indicated for regions of higher masticatory loads. More relevant for describing fracture in brittle dental ceramics and composites, properties like fracture toughness – though more and more present in advertising brochures – include additional parameters such as crack size/geometry and inverse exponential relationships,[1] more complex ideas to make sense of in practice. For many engineers and materials scientists, strength testing provides more than stress-at-failure values: strength data is a window into the nature of the microstructure, residual stresses and defect size, type and distribution in the material. Associated with fractography, strength data can guide processing routes toward eliminating strength-limiting defects and increasing material reliability.

Today, dental indirect restorative materials (i.e., reinforced glasses, glass-ceramics, polycrystalline ceramics and composites) are increasingly supplied in pre-processed block (cuboid) or blank (disc) geometries for machining in CAD/CAM systems. The processing of materials in a controlled industrial environment undoubtedly reduces possible sources of defects created during intermediary laboratorial steps (such as sintering of ceramic powders, polymerization of resin composites, etc.). This also benefits the testing of strength, once samples are sectioned from the actual components that are later placed in service. Strength testing gains thereby clinical relevance and may serve for accurate quality control.

Because many indirect materials are indicated for single-unit restorations of diminute size only (i.e., crowns, onlays, inlays), they are supplied exclusively as blocks of small dimensions, such as 18 mm × 16 mm × 18 mm^3 (e.g., C16) down to I8 blocks (8 mm × 8 mm × 15 mm^3). These limitations in size have great implications in the testing of such materials, as they fall short regarding minimal size requirements of most standards for unixial flexural strength testing using beams. Most national and international engineering standards dealing with strength testing in three-point and four-point bending set fixture spans lengths L of 40+ mm preferably, allowing a minimum of L = 20 mm, as in ASTM C 1161, ISO 17565 and ENV 843-1 for ceramics and ISO 4049 for dental resin composites. For that, at least 22 mm long beams are required, a condition not fulfilled for materials available only in the aforementioned block dimensions. To accommodate limited sized specimens, e.g., prepared out of small CAD/CAM blocks, the standard ISO 6872 for dental ceramics admits span lengths as small as 12 mm for three-point bending and 16 mm for four-point bending. The use of shorter spans in three- and four-point bending configurations is feasible not without reservations, as intrinsic problems of flexural test set-ups get amplified through miniaturization [2]. Inaccuracies in specimen-fixture articulation, positioning and parallelism, along with friction and wedging effects, as thoroughly pointed out in Refs. [3,4], may lead to several percent error in the determination of strength using regular 20 mm or 40 mm support span lengths, let alone with shorter fixtures. For miniaturized set-ups extra precision has been advised, particularly concerning alignment of loading points and refinement of testing jigs [2]. Added to these fundamental sources of error, smaller specimens are more prone to damage during production; corner chippings may be too large to be removed through chamfering of the edges, and skewed strength distributions may result thereof. This has been shown to be the case for miniaturized alumina specimens tested in Ref. [5], a problem of severe repercussions for fragile glassy dental ceramics. For resin composites, short-beam uniaxial flexural tests have also been criticized in a recent finite element analysis study due to similar shortcomings [6]. Any remark in these regards are missing in ISO 6872, a standard widely used by manufacturers to test and advertise products, and the most used standard for testing dental ceramics by the dental scientific community [7].

A resolution for small specimens is found in biaxial flexure tests, such as the piston-on-ring test, first adopted in ASTM F 394-78 for 32 mm-diameter discs under a three-ball support and later adapted for specimens having diameters between 12–16 mm in ISO 6872. Apart from allowing small-sized specimens to be tested, biaxial flexural tests benefit from edges outside any important stress field contributing to failure initiation, a common problem in uniaxial tests. The biaxial stress state developed on the tensile side of the specimen simulates to a better extent multiaxial stress conditions in real applications, and does not discriminate cracks in particular orientations. Yet, loading and support fixtures consisting of rings or multiple balls require perfectly flat parallel surfaces for the stress state to be described by the available solutions. Errors are further introduced as friction is generated between the specimen and the fixed supports.

In 2002 a new test based on a ball-on-three-balls (B3B) configuration has been devised to address some drawbacks of conventional biaxial bending tests. The set-up is based on three balls that load the specimen over one supporting ball; friction is avoided by allowing the three loading balls to roll as the specimen bends and fractures. The four contact points tolerate slight warping of the surface without invalidating the assumptions of the numerical solution. Validations against other uniaxial bending tests with various technical ceramics have attested the flexibility of the B3B test regarding specimen size and geometry. Through the use of finite element analysis

[1] Strength, σ, is inversely related to the length of pre-existing cracks or defects in the material through the Griffith/Irwin relation: $\sigma = K_{Ic}/Y\sqrt{pa_c}$, with K_{Ic} being the fracture toughness in mode I loading, Y a geometrical factor related to the crack geometry, specimen geometry and type of loading, and a_c the length of the critical crack at failure. Defects can be artificially produced by damage of components/specimens, leading to a severe drop in strength if large enough, or belong to the natural flaw population(s) of the material [1]. In ceramics natural flaws are mainly constituted of pores, inclusions (impurities), agglomerates or poorly sintered regions, usually formed during the powder processing and sintering steps. In well-controlled processing environments defects can be minimized, increasing the strength and reliability of the material, where critical crack sizes tend to scale to the size of microstructural features.

the stress state in the piece can be determined for complex 2-dimensional specimen shapes, opening the possibility for testing material samples of non-circular cross-sections.

In this contribution, we introduce the B3B method for biaxial strength testing of dental restorative CAD/CAM materials. The materials to be tested here have been thoroughly characterized in a previous contribution [8] in terms of microstructure and the elastic constants needed for the B3B test solution. Two alternatives of dealing with small CAD/CAM blocks are demonstrated herein, using either discs or rectangular specimen geometries. The solution for the function needed to calculate the biaxial strength for the plate geometry is then made available with the Poisson's ratio being the only variable to be inserted. The size effect on strength in dental CAD/CAM restoratives is further illustrated by comparing flexural strength values obtained in biaxial (B3B test) and uniaxial 4-point bending (4-PB) configurations.

2. Background

2.1. *The ball-on-three-balls (B3B) test*

The B3B test was introduced by Börger et al. [9] to overcome some disadvantages of traditional biaxial strength assemblies (i.e., ring-on-ring, piston-on-ring, piston-on-balls, etc.), highly sensitive to deviations in plane-parallelism of the specimen's faces and to the effect of unknown friction between the sample and the loading/supporting fixtures [1]. The well-defined load transfer in the B3B (four point contact) allows testing of specimens with flatness deviations up to 16% [10], and small warpings present in as-sintered specimens. The influence of friction is considerably reduced when compared to fixed supports, as the loading balls roll outward during bending of the specimen [10]. Unlike rotationally symmetric set-ups (e.g., ring-on-ring), the stress field at the tensile side of the specimen has a threefold symmetry in the B3B assembly [9]. The load is transferred through a small contact area to the specimen by the central ball, with generated tensile stresses being highly dependent upon the radius of this contact area, which is, in turn, a function of the elastic moduli of the tested material and balls [9]. Consequently, materials with low elastic modulus may show large deformations during loading that change the contact and support radii, influencing the stress state and increasing the test error. This has more severe implications for low-modulus dental composites than for stiff dental ceramics, and will be addressed in detail later in the text.

The maximum principal stress takes place at the center top of the specimen, and scales with the force applied F, and the inverse of the square root of the thickness t, viz:

$$\sigma_{max} = f(\alpha, \beta, \upsilon)\frac{F}{t^2}. \quad (1)$$

The function f, derived using finite element (FE) analysis [9], has been shown to be determined by three main independent geometrical parameters influencing the stress state in the disc (see diagram in Fig. 1a): the dimensional ratio formed by the support radius R_a (with $R_a = (2\sqrt{3}R_b)/3$), and the radius of the specimen R, (R_a/R, or β in Eq. (1)); the thickness to specimen radius ratio (t/R, or α in Eq. (1)) and; the Poisson's ratio of the tested material, ν. Accordingly, for a disc geometry with thickness t, radius R and support radius R_a, the function f can be determined using [9]:

$$f(\alpha, \beta, \upsilon) = c_0 + \frac{\left(c_1 + c_2\alpha + c_3\alpha^2 + c_4\alpha^3\right)}{1 + c_5\alpha} \times (1 + c_6\beta) \quad (2)$$

where c_i ($i = 0,\ldots 6$) are constants obtained from fitting procedures of FE analysis results. Values for these constants can be found for the range of ν ratios studied in Ref. [9], or directly calculated with a web-Mathematica tool available at www.isfk.at. This renders the B3B test scalable for small specimen sizes and different specimen geometries, only requiring some adjustment of the function f. By using rectangular plates instead of discs as specimens, the test loses the three-fold symmetry and acquires a mirror-symmetry that intersects one of the loading (supporting) points. Because the extra material on the edges of plates stiffens the specimen, an important effect on the bending strain is observed, requiring a new numerical analysis for the function f. Strength obtained using the B3B test with rectangular plates have been validated extensively for alumina, silicon nitride and a capacitor ceramic in Refs. [11,12]. Rectangular plate testing has been shown to yield values comparable to those obtained with discs described by the prediction of Weibull scaling theory.

2.2. *Size effect on strength*

Unlike fracture toughness, a material property that – in theory – should always yield the same value regardless of specimen size, geometry and testing method (at least for non-R-curve materials), strength is rather described by the distribution of flaw sizes in a set of specimens. This invariably leads to a dependence of the strength distribution on the size of the specimens and type of applied stress (i.e., uniaxial or biaxial). Implied in the Weibull theory, the most accepted statistical concept dealing with fracture of brittle materials, larger specimens have a higher probability of containing large strength-limiting defects, yielding lower strength values than small specimens tested in the same loading conditions. A direct comparison of strength values between specimens of different sizes violates this fundamental assumption and should be avoided. A solution to this problem is to scale the strengths obtained from two different specimens sizes (σ_1 and σ_2, for example) by considering their effective volumes ($V_{eff,1}$ and $V_{eff,2}$) using the well-known relation:

$$\frac{\sigma_1}{\sigma_2} = \left(\frac{V_{eff\,2}}{V_{eff\,1}}\right)^{1/m} \quad (3)$$

being m the Weibull modulus. Only through this procedure strength values obtained from different test configurations (e.g., 3- or 4-point bending) and specimens sizes using the same test set-up can be compared. The right-hand side of Eq. (3) is determined based on the location of the defect-initiating fracture in the specimens, being whether volume defects (such as pores, agglomerates) or surface defects (usually artificially-induced cracks from surface finishing procedures). If the latter

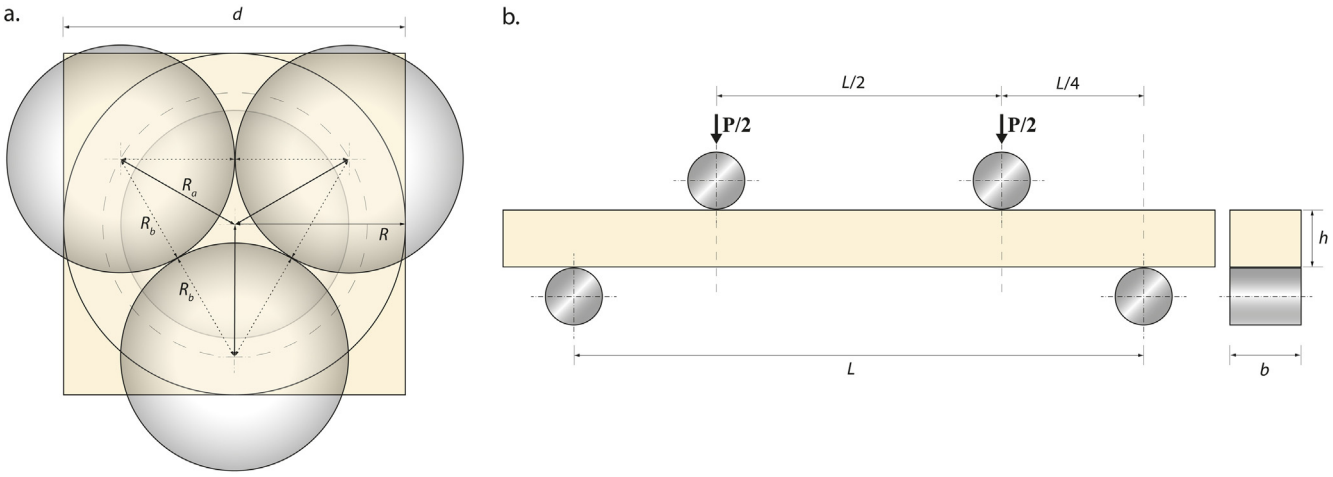

Fig. 1 – Test set-ups for the (a) B3B-test (disc and plates) seen from below (supporting ball is shaded), and for the (b) 4-point bending in a cross-sectional view.

is defining the fracture mode, V_{eff} gives room to the effective surface S_{eff}, which is also dependent on size and test geometry. Solutions for V_{eff} and S_{eff} of standardized uniaxial bending (e.g., 3- and 4-PB) assemblies have been thoroughly summarized in Ref. [13]. For the 4-PB test having the distance between the loading and supporting rollers being ¼ L (the configuration used in the present study, see Fig. 1b), V_{eff} and S_{eff} are determined by:

$$V_{eff,4PB} = \frac{V}{4}\left[\frac{(m+2)}{(m+1)^2}\right] \quad (4)$$

and

$$S_{eff,4PB} = L\,[h + b\,(m+1)]\left\{\frac{(m+2)}{\left[2(m+1)^2\right]}\right\} \quad (5)$$

where V is the specimen's volume ($b \times h \times L$) and m the Weibull modulus. The effective volume, V_{eff}, in discs and plates tested using the B3B test takes place at the center of the top surface and is determined by [14]:

$$V_{eff,B3B} = \int_{\sigma>0}\left(\frac{\sigma_{eq}(\vec{r})}{\sigma_{ref}}\right)^m d^3r \quad (6)$$

where $\vec{r}$ is the position vector and σ_{ref} is taken to be equal to the maximum tensile principal stress in the specimen, that is, $\sigma_{ref} = \sigma_{max}$. The S_{eff} for the B3B specimens is given by:

$$S_{eff,B3B} = \int_{\sigma>0}\left(\frac{\sigma_{eq}(\vec{r})}{\sigma_{ref}}\right)^m dS. \quad (7)$$

For the B3B-tests, this integration has to be performed numerically.

3. Materials and methods

3.1. *Materials and specimen preparation*

The materials used in the present study were selected in order to span over a wide spectrum of restoratives classes currently available in the market. Therefore, a 3 mol% yttria-stabilized tetragonal zirconium dioxide material (e.max ZirCAD), a lithium disilicate (e.max CAD), two lithium silicate/phosphate glass-ceramics (Suprinity and Celtra Duo), a leucite-based (Empress CAD), feldspar-reinforced aluminosilicate glass (Vitablocs Mark II), a polymer-infiltrated reinforced-glass network (Enamic) and a nano-particulate prepolymerized resin composite (Lava Ultimate) were included. Their composition, microstructure and elastic properties were comprehensively described recently in Ref. [8]. Those properties relevant to the present work are summarized in Table 1.

Five CAD/CAM blocks of each material with dimensions approx. $14 \times 12 \times 18\,mm^3$ (e.g., C14, I14) were ground with a fine diamond wheel (D50) to obtain square cross-sections of $12 \times 12\,mm^2$ for the later sectioning of plates, or ground with a fine diamond bur (Ceratec, Kreuztal-Kredenbach, Germany) to obtain circular (Ø = 12 mm) cross-sections for the production of discs. Seven slices with thickness 1.50 ± 0.05 mm were cut from each block using a precision cutting machine (IsoMet 5000, Buehler, Illinois, USA) under water irrigation. Following the manufacturer's instructions, Suprinity and e.max CAD specimens underwent a crystallization firing for 8 min at 840 °C (heating rate 55 °C/min) or 10 min at 850 °C (heating rate 30 °C/min), respectively. The specimens were positioned inside the oven (Vacumat 4000, Vita Zahnfabrik, Bad Säckingen, Germany) on top of a porous refractory material that allowed homogeneous heat distribution through the thickness. During the cooling phase, the furnace was kept closed until 680 °C was reached. The oversized discs and plates were then ground parallel on both sides with a diamond wheel and mirror polished on one side with SiC grinding paper (P600 down to P4000) in an automatic polishing machine (Phoenix Beta Vector 60-1990, Buehler, Illinois, USA) under constant water irrigation to a final thickness of 1.20 ± 0.05 mm. The

Table 1 – Evaluated materials, their class and elastic properties relevant for this study.

Material	Manufacturer	Class	Young's modulus E (GPa)[a]	Poisson's Ratio υ[a]
e.max ZirCAD	Ivoclar-Vivadent	3 mol% yttria-stabilized tetragonal zirconia polycrystals (3Y-TZP)	205.2	0.243
e.max CAD	Ivoclar-Vivadent	Lithium disilicate (LS_2) glass-ceramic	102.7	0.215
Celtra Duo	Dentsply DeTrey	Fully-sintered lithium silicate/Phosphate (LSP) glass-ceramic	107.9	0.222
Suprinity	VITA Zahnfabrik	Pre-sintered Lithium Silicate/phosphate (LSP) glass-ceramic	104.9	0.208
Vitablocs Mark II	VITA Zahnfabrik	Feldspar-reinforced aluminosilicate glass (FAG)	71.3	0.231
Empress CAD	Ivoclar-Vivadent	Leucite-based glass-ceramic (LG)	65.5	0.204
Enamic	VITA Zahnfabrik	Polymer-infiltrated particle-reinforced-glass network (PIRGN)	37.8	0.244
Lava Ultimate	3M ESPE	Nano-particulate pre-polymerized resin composite (RC)	12.7	0.45

[a] Values of Elastic modulus and Poisson's ratio were obtained from Ref. [8] as the average of the values from the Resonant Beam Technique (RBT) and Resonant Ultrasound Spectroscopy (RUS). The exception was the values for Lava Ultimate, which were taken from the results of the RBT method, which were more reliable.

quality of the surface polish was measured for 10 specimens per group with a high resolution confocal optical profilometer (CT 100, CyberTechnologies, Germany) with x–y step-sizes of 5 μm and a vertical resolution of 0.02 μm. A mean roughness depth (R_z) of 0.5 ± 0.1 μm was measured for all materials. Specimens for the 3Y-TZP groups were cut from green blocks (15.4 × 19 × 39 mm^3, i.e., B40 L), previously ground to square (15 × 15 mm^2) or circular (Ø = 15 mm) cross-sections. The pre-sintered e.max ZirCAD slices were wet polished with SiC paper (P2500) and further sintered for 2 h at 1530 °C (heating rate of 200 °C/h). Their final dimensions were 12 × 12 × 1.20 mm for the rectangular plates, and 12 × 1.20 mm for the discs, with a mean R_z of 0.8 ± 0.2 μm. Thirty specimens for each geometry (discs/plates) and material were produced, except for Lava Ultimate, for which only plates were produced (n = 30).

Beams for testing in 4-point bending (4-PB) were cut from larger CAD/CAM blocks, commercially available for the materials e.max CAD (14.5 × 14.5 × 32 mm^3, i.e., B32), Vitablocs Mark II (15.5 × 19 × 39 mm^3, i.e., I-40/19), as well as for e.max ZirCAD (B40 L) (n = 30). The specimens for the latter were cut and polished (Grit 2500) down to 2.5 × 3.2 × 25 mm^3 in order to compensate the sintering shrinkage (20%), whereas beams for e.max CAD and Vitablocs Mark II were sectioned and ground parallel to their final dimensions (2 × 2.5 × 25 mm^3). E.max CAD beams were crystallized following the same protocol as described for discs and plates. The lower side surface (to be later subjected to bending) of e.max CAD and Vitablocs Mark II was mirror polished following the same protocol as used for the biaxial strength specimens (P600–P4000). Similar R_z values to those of their B3B counterparts were measured. The edges of the polished side were chamfered with SiC paper (P2500) in order to remove preparation defects. Specimens containing edge defects were eliminated. An overview of the different specimen geometries test set-ups is presented in Fig. 2.

3.2. *Mechanical testing and strength determination*

The B3B test was conducted using two especially designed assemblies (see Fig. 2b). Prior to testing, the dimension d of the specimens was carefully measured in order to obtain R (=d/2) using a digital hand micrometer with resolution 0.002 mm (293-521-30, Mitutoyo Corp, Japan). The thickness of the B3B specimens was measured at their center with a rounded-tip digital dial gage also with resolution 0.002 mm (ID-C112XB, Mitutoyo, Japan). Support and loading balls with the same radius (R_b = 4 mm) were used. Specimens were tested in a universal testing machine (Z2.5, Zwick, Ulm, Germany). A preload of 10 N was applied before the positioning aid was removed, which allowed the supporting balls to roll free upon bending/fracture of the specimen. The tests were conducted at cross-head speeds ranging between 0.5 and 1.5 mm/min to minimize slow crack growth (fracture took place within 5–15 s). After fracture, the specimen's fragments were carefully collected and their number registered. The biaxial strength was calculated using Eqs. (1) and (2) for the disc specimens, whereas a new FE analysis had to be conducted to derive the f function needed to solve Eq. (1). For the specific plate dimensions (i.e., 12 × 12 mm^2) and assembly dimensions used in the present study, f reads:

$$f(\tau,\nu) = 0.323308 + \frac{(1.30843 + 1.44301\,\nu)\times\left(1.78428 - 3.15347\,\tau + 6.67919\,\tau^2 - 4.62603\,\tau^3\right)}{1 + 1.71955\,\tau} \quad (8)$$

where $\tau = t/R_a$. Conversely to Eq. (2), this f function for the plate geometry needs only two variables to be inserted, the ratio t/R_a varying for each specimen (due to variations in thickness), and the Poisson's ratio varying for each material.

The uniaxial flexural strength of beams was determined using a 4-point ¼-point bending fixture (Fig. 1b), with outer and inner span lengths 20 and 10 mm, respectively. Fully-articulated support and loading rollers were used to avoid not considered stress concentrations during the test (Fig. 2c). Specimen's dimensions (width b, thickness h) were determined with 0.002 mm precision using a digital gage. Testing was carried out in a universal testing machine (Dyna-Mess Prüfsysteme, Stolberg, Germany), at a cross-head speed of 0.1 mm/s

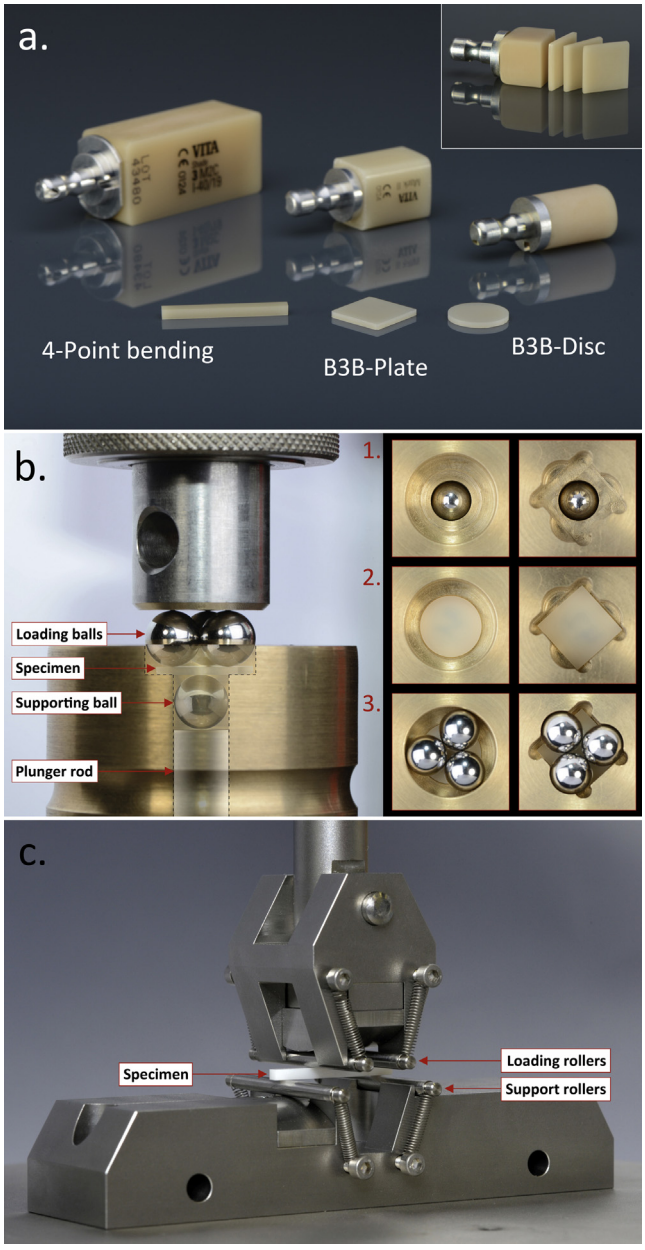

Fig. 2 – Specimens and loading assemblies used for strength determination. In (a) CAD/CAM blocks in original size with respective specimen geometries are shown for the B3B and 4-PB tests. In (b) the B3B test configuration is illustrated. Steps 1–3 refer to the placement of the loading ball onto the plunger rod (under the specimen), the insertion of the specimen with its tensile (polished) side upwards, and the placement of the supporting balls into the guide, respectively. Note how the loading balls touch each other and cannot change position before the specimen is pre-loaded. In (c) the 4-PB fixture is presented. Fully-articulated support and loading rollers hinder unwanted stress concentrations during the test.

(specimens fractured within 5–10 s). The flexural strength was calculated using:

$$\sigma_{4PB} = \frac{3FL}{4bh^2}. \quad (9)$$

The strength data obtained using the B3B (disc and plate) and 4-PB was analyzed using Weibull statistics in order to obtain the characteristic strength (σ_0) and Weibull modulus (m) through the Maximum Likelihood estimation procedure [15], as well as their confidence intervals (90%) for each material and specimen geometry. The effective volume (V_{eff}) and effective surface (S_{eff}) were calculated for the B3B and 4-PB specimens using the equations described in Section 2.2. In order to allow comparison between the strength data of the two different loading configurations (biaxial stress state in the B3B vs. uniaxial stress condition in the 4-PB), an equivalent stress state was calculated for the B3B results using the Principle of Independent Action (PIA) [16]:

$$\sigma_{eq,PIA} = (\sigma_I{}^m + \sigma_{II}{}^m + \sigma_{III}{}^m)^{1/m} \quad (10)$$

where σ_I, σ_{II} and σ_{III} are the principal stress components.

3.3. *Fractographic analysis*

The fragments of the weakest specimens of each group were examined under a stereomicroscope (SV 6, Zeiss Germany) equipped with an external light source and further gold sputtered for observation under SEM (Leitz ISI-SR-50, Akashi, Japan) to detect fracture modes that would invalidate the test (e.g., fractures arising from cone cracks developed around the supporting ball). A full fractographic evaluation of fracture modes and nature of defects was not conducted due to the enormous work that it would involve.

4. Results and discussion

Characteristic strength values obtained using the B3B test for disc and plate geometries, as well as under 4-PB for e.max ZirCAD, e.max CAD and Vitablocs Mark II, are listed in Table 2 along with respective Weibull modulus m. The strength values measured for the tested dental CAD/CAM restoratives have shown to span over a wide interval, from 100 MPa for the feldspar-reinforced aluminosilicate glass, up to 1300 MPa for the 3Y-TZP. High-content glass materials (e.g., Vitablocs Mark II, Empress CAD) and composites (e.g., Enamic, Lava Ultimate) form the lower quarter, with the high-crystalline content lithium-based glass-ceramics defining the intermediate range, and the polycrystalline e.max ZirCAD setting the upper bound. The Weibull modulus, a measure of the data scatter (and therefore of the material's reliability) has shown high values for most materials, usually over 10, surpassing the benchmark of 20 with Vitablocs Mark II. The high m values reflect the advanced technological stage in the fabrication and processing of pre-sintered or fully-sintered ceramic-based blocks for dental restorations. The production of such pre-processed blocks for biomedical applications is a relative new engineering field, involving fundamental processing knowhow from the glass and ceramic industries,

Table 2 – Characteristic strength (σ_0) and Weibull modulus (m) and respective 90% confidence intervals for B3B-Disc, B3B-Plate and 4-PB.

Material	Test geometry	σ_0 (MPa) [90% C.I.]	m [90% C.I.]
e.max Zir-CAD	B3B-Disc	1240.89 [1216.59–1265.94]	16.91 [12.66–20.62]
	B3B-Plate	1303.21 [1268.40–1339.38]	12.30 [9.20–15.10]
	4-PB	1030.30 [1004.40–1057.17]	13.10 [9.80–16.00]
e.max CAD	B3B-Disc	647.98 [635.69–660.65]	17.45 [13.07–21.29]
	B3B-Plate	609.80 [594.78–625.38]	13.40 [10.00–16.30]
	4-PB	462.06 [446.85–477.96]	10.00 [7.50–12.20]
Celtra Duo	B3B-Disc	626.84 [587.74–669.02]	5.19 [3.89–6.33]
	B3B-Plate	565.80 [534.02–599.86]	5.80 [4.30–7.10]
Suprinity	B3B-Disc	611.24 [573.80–651.58]	5.29 [3.96–6.45]
	B3B-Plate	537.03 [503.77–572.89]	5.20 [3.90–6.40]
Vitablocs Mark II	B3B-Disc	118.78 [116.67–120.94]	18.72 [14.02–22.83]
	B3B-Plate	118.65 [116.68–120.68]	19.90 [14.90–24.30]
	4-PB	110.93 [109.54–112.35]	26.50 [19.80–32.30]
Empress CAD	B3B-Disc	199.45 [195.70–203.31]	17.62 [13.20–21.48]
	B3B-Plate	187.77 [183.92–191.74]	16.10 [12.10–19.70]
Enamic	B3B-Disc	195.67 [192.31–199.13]	19.28 [14.44–23.51]
	B3B-Plate	193.45 [190.04–196.95]	18.80 [14.10–23.00]
Lava Ultimate	B3B-Plate	300.64 [291.52–310.15]	10.90 [8.10–13.20]

like milling/powder technology and sintering routes to obtain dense, homogeneous monolithic stress-free blocks.

An apparent reservation to this remark concerns the lithium silicate/phosphate glass-ceramics developed by the companies Vita and Dentsply in conjunction with the Fraunhofer Institute for Silicate Research in Germany and marketed separately under different product brands, i.e., Suprinity® and Celtra®. Both products are supplied either as partially-crystallized glass precursor or as fully-crystallized glass-ceramic blocks. One of each of these two forms was chosen for testing herein, namely Suprinity and Celtra Duo. The partially-crystallized form should provide ease of machining, requiring an extra firing (crystallization) step to be conducted chairside. In this sense, the damage induced to the fragile glassy block by diamond-coated grinding instruments during machining is a source of concern. During preparation of specimens for this study, a whole set of specimens sectioned using a used diamond saw were discarded due to macroscopic cracks running from the edges to the interior of the discs/plates. This was also observed for the partially-crystallized e.max CAD blocks, but to a lesser extent. The use of a new blade prevented the occurrence of such cracks. This problem was not observed for Celtra Duo or any other material. Although the same crystalline and glass phase composition was confirmed for crystallized Suprinity and Celtra Duo in the first contribution of this series using Raman spectroscopy and X-ray diffraction, Celtra Duo showed larger Li_2SiO_3 crystallites (~1 μm) than Suprinity (~0.5 μm). The industrial crystallization of Celtra Duo most probably differs (regarding time, temperature) from that recommended for the Suprinity glassy blocks (chairside crystallization firings need to be fast for productivity purposes). Despite the trend of slightly lower strength values measured for Suprinity compared to Celtra Duo, no significant differences in terms of strength can be stated between both materials. Quite surprisingly, the lithium silicate/phosphate glass-ceramic reached strength values comparable to those of the lithium disilicate e.max CAD. On the other side, an extremely low Weibull modulus (~5.5) was found for both Suprinity and Celtra Duo, suggesting a common source of material-dependent strength-limiting defects of wide size distribution. SEM evaluation of etched samples revealed the presence of multiple cracking and surface pitting distributed over the entire specimen surface (see Fig. 3), found in both materials. The consequence is a high variation in strength values. In the case of Suprinity, for example, measured values ranged from 278 up to 769 MPa. These defects were not induced by specimen preparation, but suggest rather a severe thermal incompatibility between phases (3 crystal phases + 1 glass phase containing dissolved ZrO_2), supposedly resulting in high magnitude of local residual stresses that are relieved during cooling by means of micro-cracking. The surface pits result from the coalescence of cracks, being washed-out during etching. Without speculating further, the processing of this material clearly needs improving, showing nevertheless potential if the abovementioned problem is eliminated.

The use of rectangular plates as alternative to using disc-shaped specimens for biaxial testing has shown to be appropriate for the testing of flexural strength of dental materials and offers a convenient solution for materials supplied as blocks. The numerical solution however, differs from that of discs due to changes in the stress state in the plate resulting mainly from the stiffening effect of the extra material at the edges. Here an easy-to-apply solution is given (Eq. (8)), with the Poisson's ratio as the only material parameter to be inserted. However, Eq. (8) can only be applied for the exact positioning of the specimen with relation to the supporting radius used in this study (the jig contained two guide walls that helped to keep the plate specimens in this particular position). Larger plates could be used, but these two sides at 90° must follow this specific positioning.

Multiple fracture pieces result from the fracture event due to the high stored strain energy, and a positive correlation is

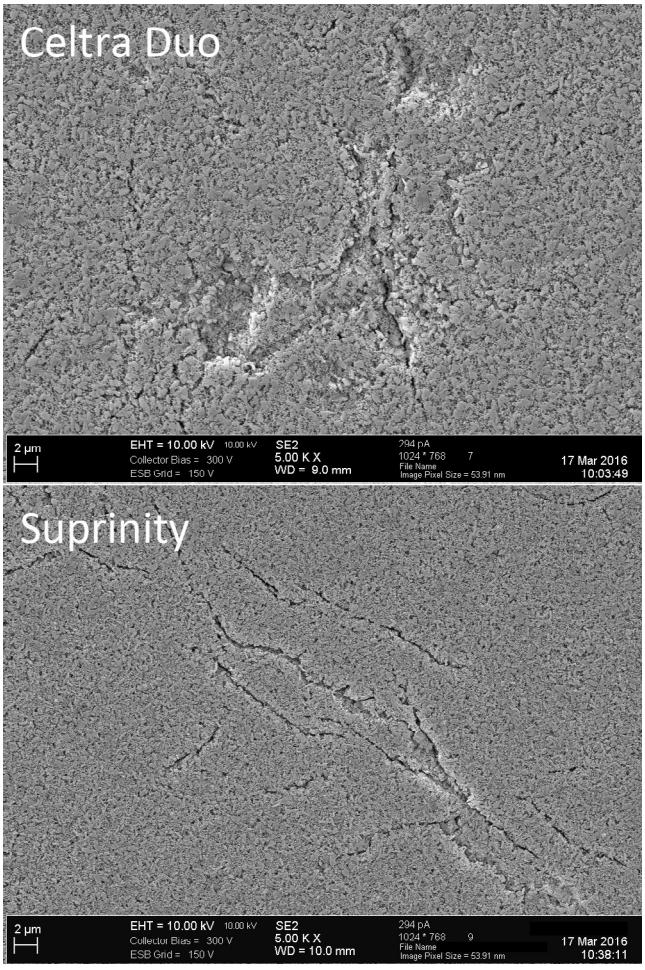

Fig. 3 – Etched surfaces (0.5% HF, 30 s) of broken specimens of Celtra Duo and Suprinity showing surface defects and multiple cracking. Both features were found for both materials in the same extent. These defects were probably responsible for the low Weibull modulus measured.

usually observed between fractured pieces and strength values [17]. For some of the tested materials this relation was more evident than for others; in Fig. 4 fractured specimens are shown in two specimen shapes for two different materials.

Both volume and surface experiencing stress amplitudes for the initiation of critical cracks is higher for the larger beams measured under 4-PB than for the biaxial specimens. Expectedly, strength values were significantly lower under uniaxial bending, just as predicted for Weibull materials (Fig. 6). The Weibull modulus might not differ significantly from one test configuration to the other though, provided that the flaw population is uniformly distributed in the same manner in both specimen sizes. The size effect of strength is demonstrated for dental ceramics herein by means of specimens of different sizes tested in uniaxial (4-PB) and biaxial (B3B) bending. In Tables 3 and 4 the strength of biaxial specimens is given as the equivalent strength in uniaxial bending via Eq. (10) for e.max ZirCAD, e.max CAD and Vitablocs Mark II, along with their effective volume and surface, respectively. The effect of the Weibull modulus becomes evident; materials with higher m show lower V_{eff} and S_{eff}, as was the case for Vitablocs Mark II.

The size effect is better visualized in Fig. 7, where the lines are the extrapolations of the Weibull theory for effective surface based on the 4-PB results. The better fitting of the data points for the B3B-test within the confidence intervals indicate if volume or surface defect models are more appropriate for describing the fracture behavior of the materials. In Fig. 7 only the relation between strength and the effective surface is shown, due to a better fit in comparison to the effective volume, for all three materials. The slope is the inverse of the Weibull modulus being steeper for e.max CAD and e.max ZirCAD than for Vitablocs Mark II. For e.max ZirCAD and e.max CAD the B3B strength values are consistent with the 4-PB values in the framework of the Weibull theory. For Vitablocs Mark II the B3B and 4-PB results did not coincide, which gives room to speculations regarding the nature, orientation and distribution of defects responsible for fracture depending on the test configuration used. A thorough fractographic analysis of Vitablocs Mark II conducted by Quinn et al. [19] on 4-PB speci-

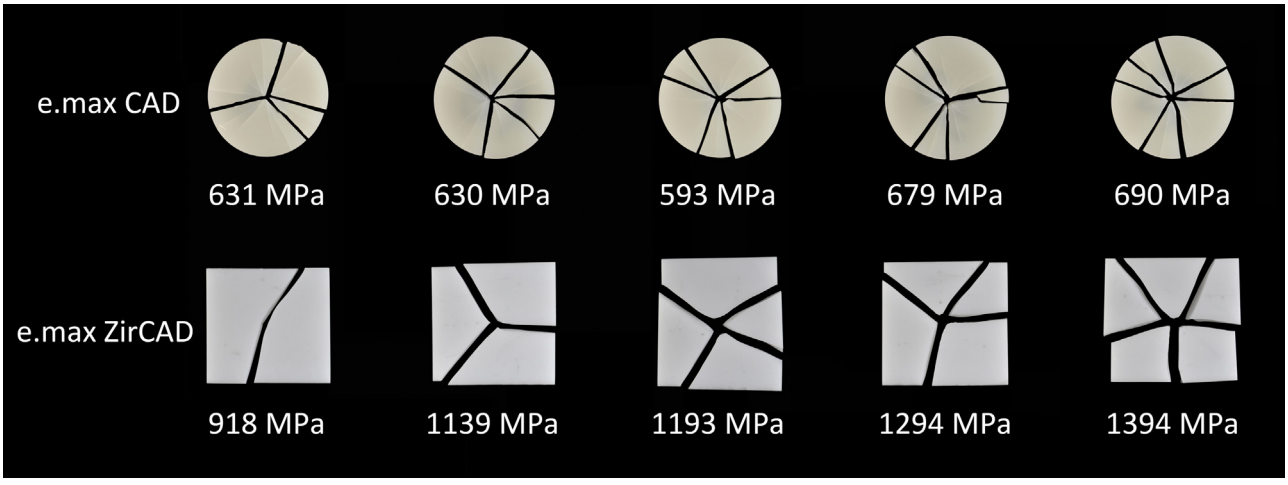

Fig. 4 – Fractured specimens in disc and rectangular plate geometries. The number of fractured pieces increased with the stress at failure.

Table 3 – Characteristic strength (σ_0), effective volume (V_{eff}) and equivalent strength ($\sigma_{eq,PIA}$) for the three test geometries.

Material	B3B-Disc			B3B-Plate			4-PB	
	σ_0 (MPa)	V_{eff} (mm^3)	$\sigma_{eq,PIA}$ (MPa)	σ_0 (MPa)	V_{eff} (mm^3)	$\sigma_{eq,PIA}$ (MPa)	σ_0 (MPa)	V_{eff} (mm^3)
e.max ZirCAD	1240.89	0.0124	935.36	1303.21	0.0240	907.00	1030.30	1.8252
e.max CAD	647.98	0.0084	482.80	609.80	0.0198	433.10	462.06	2.5339
Vitablocs Mark II	118.78	0.0081	90.44	118.65	0.0069	91.16	110.93	0.9742

Table 4 – Characteristic strength (σ_0), effective surface (S_{eff}) and equivalent strength ($\sigma_{eq,PIA}$) for the three test geometries.

Material	B3B-Disc			B3B-Plate			4-PB	
	σ_0 (MPa)	S_{eff} (mm^2)	$\sigma_{eq,PIA}$ (MPa)	σ_0 (MPa)	S_{eff} (mm^2)	$\sigma_{eq,PIA}$ (MPa)	σ_0 (MPa)	S_{eff} (mm^2)
e.max ZirCAD	1240.89	0.4833	976.88	1303.21	0.6631	960.65	1030.30	27.0620
e.max CAD	647.98	0.3800	507.01	609.80	0.6006	457.39	462.06	29.4710
Vitablocs Mark II	118.78	0.3797	94.52	118.65	0.3313	95.07	110.93	26.7990

mens revealed intrinsic volume flaws (mainly microstructural heterogeneities and pores) as the nature of strength-limiting defects, leading to a Weibull modulus $m = 35$ and $\sigma_0 = 119$ MPa if grinding and corner flaws were to be disregarded. In our experiments $\sigma_{eq,PIA}$ and m modulus were significantly higher for 4-PB specimens in comparison to B3B, which diverges from the expected Weibull behavior. Without a deeper fractographic analysis we can only rely on speculation, but it seems probable that these differences might have resulted from the fact that I14 blocks were used for producing B3B specimens, and I40 blocks for 4-PB specimens. Apparently, the processing routine for these two blocks sizes differs to a sufficient extent to alter the distribution of defects inside the volume of the blocks: the materials in I14 and I40 blocks are chemically the same, but not defectwise. Added to that, the orientation of sectioning (orthogonal to the long axis of the block for the B3B specimens, and parallel for 4-PB) might have exposed the surface of the specimens to different defect orientations, considering that the powder of this material is uniaxially pressed before sintering. This was not the case for e.max ZirCAD since both specimen geometries were cut out of B40 L blocks. For e.max CAD different block sizes were used for the two different specimen geometries, and the fit to the Weibull behavior indicates comparable defect distributions in both block sizes.

A very good agreement between biaxial strength results using discs and plates is seen for Vitablocs Mark II, Enamic, Empress CAD and Celtra Duo (Fig. 5). For the other tested materials the 90% confidence intervals nearly overlapped. A note of caution: although the data points and confidence interval ranges in Fig. 5 aid in the quick comparison of strength values obtained for discs vs. plates, differences in V_{eff} and S_{eff} via Eqs. (6) and (7), as shown in Tables 3 and 4 (mainly due to differences in σ_0, m and specimen geometry), demand an analysis of the size effect, as conducted above for the materials tested under 4-PB and B3B (see Eq. (3)). Following this procedure, the strength of discs were equivalent to the strength of plates, for all materials (not shown).

Those materials that showed a higher variation in strength values from disc to plate in the B3B test have a very fine microstructure in common (~2 μm crystal size for e.max CAD, and crystallites and grains <1 μm for Suprinity and e.max ZirCAD). High modulus materials tend to have a very narrow defect size distribution with defect size approaching the length scale of the microstructure. That makes them more

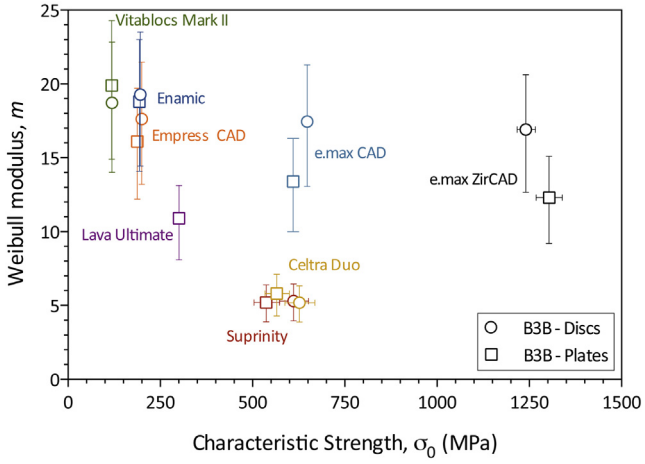

Fig. 5 – Weibull modulus *m* vs. characteristic biaxial strength for disc (circle) and plate (square) geometries tested using the B3B test according to material.

susceptible to the introduction of artificial defect populations, such as surface scratches from finishing and polishing procedures, which will in turn act as fracture initiation sites and increase the scatter of strength values [18]. Fractography could help to characterize the type of fracture mode [17]. For such materials, a higher number of test specimens is advised as well as a very strict specimen preparation procedures.

Both test geometries, the B3B-test as well as the 4-point bending test have been designed to be used with specimens that deflect only very little during the test. As indicated above, the deflection leads to a reduction of the support radius (or—in a bending test of the support span). A neglection of this fact, as is usually done during the evaluation of the test, leads to a systematic overestimation of strength. The magnitude of deflection during a bending test is governed by the applied force at fracture and Young's modulus of the material. The figure of merit to characterize deflection is thus $ME = \sigma_f/E$, fracture strength over Young's modulus. The higher σ_f/E, the higher is the deflection at fracture for a given ratio specimen thickness over support radius (B3B-test) or span length (4PB). Following ideas developed previously [3,20], this systematic error was evaluated for the materials and tests used in this study. Regarding ME, we make distinction between three

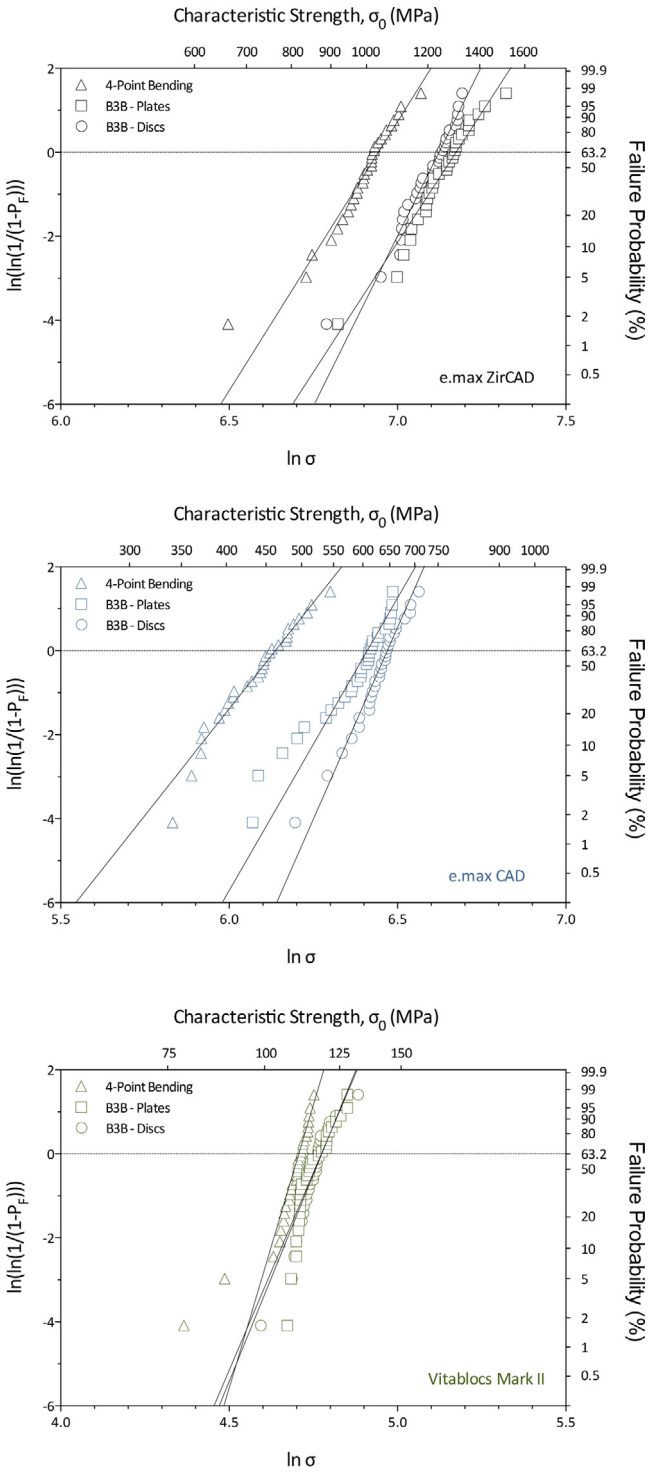

Fig. 6 – Weibull plots of e.max ZirCAD, e-max CAD and Vitablocs Mark II comparing the strength distribution for specimens tested under biaxial (B3B discs and plates) and uniaxial (4-PB) bending. Note the lower characteristic strength measured using the 4-PB configuration.

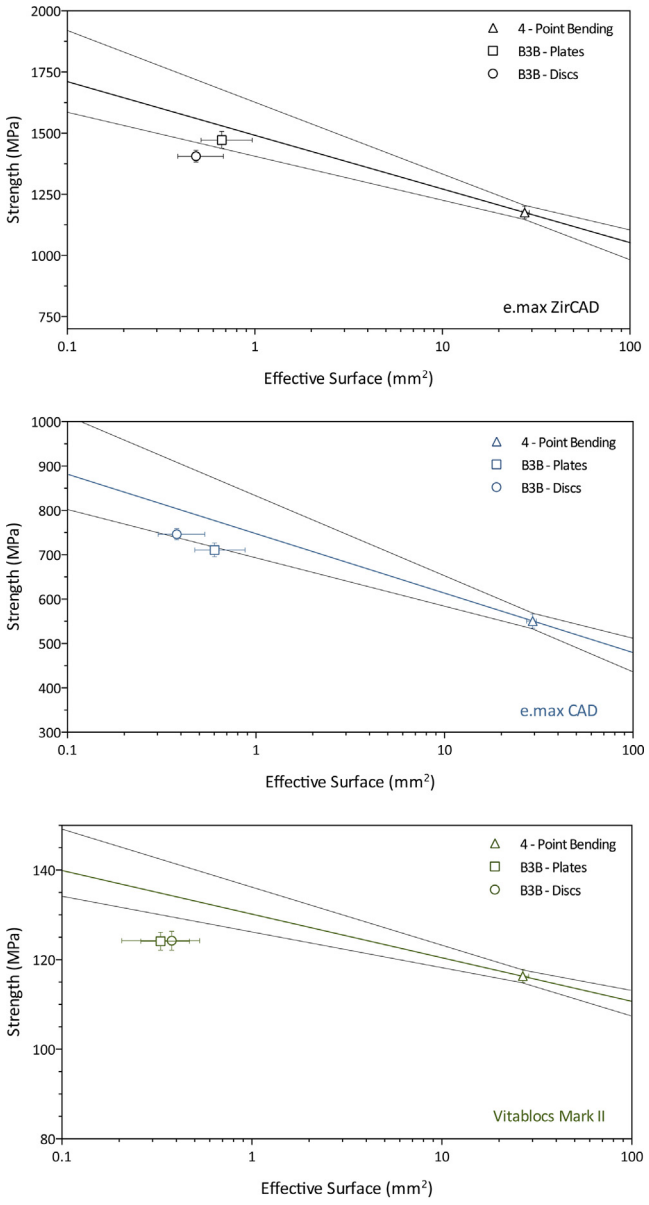

Fig. 7 – Plot Strength vs. Effective Surface (S_{eff}) for e.max ZirCAD, e-max CAD and Vitablocs Mark II. Note how for e.max ZirCAD and e.max CAD the B3B results coincide (overlapping with 90% C.I.) with the extrapolation of the Weibull theory based on the 4-PB data.

groups of materials with ME ≈ 1×10^{-3} to 2×10^{-3} (Vitablocs Mark II, Empress CAD), ME ≈ 5×10^{-3} to 6×10^{-3} (e.max ZirCAD, e.max CAD, Suprinity, Celtra Duo and Enamic) and ME ≈ 24×10^{-3} (Lava Ultimate), respectively. For the first group the overestimation of strength is neglectable for B3B-tests and 4-point bending test. For the second group the overestimation is in the order of 2.5–3% for the B3B-tests and 0.5–1% for the 4-point bending test, while it is approximately 5% for both test types for group three (Lava Ultimate). This indicates that also with respect to the test precision the biaxial test geometries are suitable for testing dental materials such as dental composites. Since this error is a systematic overestimation, it will not corrupt the interpretation of the scatter of strength. A fair comparison of materials will be possible.

5. Conclusions

Outside of the academic sphere, dentists are bombarded with data in advertising brochures for new products reporting results from diverse mechanical tests, prone to misleading interpretations. Many make use of miniaturized fixtures for uniaxial bending disregarding the high testing sensitivity; some employ the biaxial test solution for specimens with geometries other than discs disregarding the validity of the numerical solution. Clearly, it is time for better standardization when testing mechanical properties of dental materials. We demonstrated here the possibility of using plates under biaxial flexure in conjunction with the B3B test in order to facilitate the testing of materials supplied as small CAD/CAM blocks. Both B3B test geometries, rectangular plates and round discs have shown to be equally suitable and yield similar strength values for the same support radius. It becomes clear from our results that the size effect and the test configuration render very different nominal strength values when testing brittle materials such as dental restoratives. A proper analysis is therefore mandatory on the basis of the Weibull theory for brittle fracture.

Acknowledgement

All materials were kindly donated by the manufacturers.

REFERENCES

[1] Danzer R. On the relationship between ceramic strength and the requirements for mechanical design. J Eur Ceram Soc 2014;34:3435–60.
[2] Lube T, Manner M, Danzer R. The minituarization of the 4-point-bend test. Fatigue Fract Eng Mater Struct 1997;30:1605–16.
[3] Baratta FI, Matthews WT, Quinn GD. Errors associated with flexure testing of brittle materials. Report no. MTL TR 87-35. US Army Materials Technology Laboratory; 1987.
[4] Quinn GD, Morell R. Design data for engineering ceramics: a review of the flexure test. J Am Ceram Soc 1991;74:2037–66.
[5] Lube T, Manner M. Development of a bending-test device for small samples. Key Eng Mater 1997;132–136:488–91.
[6] Pick B, Meira JBC, Driemeier L, Braga RR. A critical view on biaxial and short-beam uniaxial flexural strength tests applied to resin composites using Weibull, fractographic and finite element analysis. Dent Mater 2010;26:83–90.
[7] Della Bona A, Dal Bello Y, Sartoretto SC. Use of standards in papers published in dental journals. Braz Dent J 2012;23:471–6.
[8] Belli R, Wendler M, de Ligny D, Cicconi MR, Petschelt A, Peterlik H, et al. Chairside CAD/CAM materials. Part 1: measurement of elastic constants and microstructural characterization. Dent Mater 2016, http://dx.doi.org/10.1016/j.dental.2016.10.009.
[9] Börger A, Supancic P, Danzer R. The ball on three balls test for strength testing of brittle discs: stress distribution in the disc. J Eur Ceram Soc 2002;22:1425–36.
[10] Börger A, Supancic P, Danzer R. The ball on three balls test for strength testing of brittle discs: Part II: analysis of possible errors in the strength determination. J Eur Ceram Soc 2004;24:2917–28.
[11] Danzer R, Supancic P, Harrer W. Biaxial tensile strength test for brittle rectangular plates. J Ceram Soc Jpn 2006;114:1054–60.
[12] Harrer W, Danzer R, Supancic P, Lube T. The ball on three balls test: strength testing of specimens of different sizes and geometries. Proc. 10th ECerS Conf 2007:1271–5.
[13] Quinn GD. Weibull strength scaling for standardized rectangular flexure specimens. J Am Ceram Soc 2003;86:508–10.
[14] Munz D, Fett T. Ceramics: mechanical properties, failure behavior, materials selection. Berlin, Heidelberg: Springer-Verlag; 1999.
[15] EN-843-5. Mechanical testing of monolitic ceramics at room temperature. Part 5: Statistical treatment; 1997.
[16] Freudenthal A. A statistical approach to brittle fracture. Fracture Academic Press; 1968. p. 591–619.
[17] Harrer W, Morell R, Danzer R. Fractography of biaxial tested Si3N4-specimens. J Eur Ceram Soc 2014;34:3283–9.
[18] Harrer W, Danzer R, Morell R. Influence of surface defects on the biaxial strength of a silicon nitride ceramic—increase of strength by crack healing. J Eur Ceram Soc 2012;32:27–35.
[19] Quinn GD, Hoffman K, Quinn JB. Strength and fracture origins of a feldspathic porcelain. Dent Mater 2012;28.
[20] Danzer R, Supancic P, Harrer W. Der 4-Kugelversuch zur Ermittlung der biaxialen Biegegestigkeit spröder Werkstoffe. In: Kriegsmann Jochen, editor. Technische keramische Werkstoffe. Ellerau: HvB Verlag GbR; 2009. p. 1–48.